(13) R. R. Holmes, *Acc. Chem. Res.*, **5**, 296 (1972).
(14) L. S. Bartell and K. W. Hansen, *Inorg. Chem.*, **4**, 1777 (1965).
(15) R. J. Gillespie, *Inorg. Chem.*, **5**, 1634 (1966).
(16) R. Wolf and R. Weiss, personal communication.
(17) H. Oberhammer and R. Schmutzler, *J. Chem. Soc., Dalton Trans.*, 1454 (1976).
(18) A. Strich and A. Veillard, *J. Am. Chem. Soc.*, **95**, 5574 (1973).
(19) K. W. Hansen and L. S. Bartell, *Inorg. Chem.*, **4**, 1775 (1965).
(20) D. D. Swank, C. N. Caughlan, F. Ramirez, and J. F. Pilot, *J. Am. Chem. Soc.*, **93**, 5236 (1971).
(21) Derivative II which has saturated rings should have more TP character than I if the arguments referred to[3] here apply. The percent displacement[8] shows the opposite, however. As discussed in ref 5 and 6, intermolecular hydrogen bonding in II is responsible for the reversal. The molecules are so positioned in the unit cell that N—H···O hydrogen bonding acts to open the $N_{eq}$–P–$N_{eq}$ angle. Although hydrogen bonding is present in I, the positioning of the neighboring oxygen atoms does not induce an appreciable effect of this type. Computer minimization via molecular mechanics bears this out.[5]
(22) J. R. Devillers and R. R. Holmes, *J. Am. Chem. Soc.*, **99**, 3332 (1977).

---

Contribution from the Fachbereich Naturwissenschaften II,
Gesamthochschule, 5600 Wuppertal, West Germany

# Crystal and Molecular Structure, Reinvestigated Vibrational Spectra, and Normal-Coordinate Analysis of Potassium (Trifluoromethyl)trifluoroborate, $K[CF_3BF_3]$[1]

D. J. BRAUER, H. BÜRGER,* and G. PAWELKE

*Received January 12, 1977* AIC70015V

The structure and vibrational spectra of $K[CF_3BF_3]$ have been determined by x-ray diffraction methods and have been reinvestigated by IR and Raman spectroscopy, respectively. The compound crystallizes in the monoclinic space group $C_{2h}^5$-$P2_1/c$ with $a = 4.843$ (1) Å, $b = 16.331$ (4) Å, $c = 6.348$ (2) Å, $\beta = 101.89$ (3)°, $Z = 4$, $d_c = 2.378$ g cm$^{-3}$, and $d_o = 2.5$ (1) g cm$^{-3}$. The structure was refined anisotropically to a conventional $R$ factor of 0.058 based on 767 counter measured, absorption corrected reflections with $|F_o| > 4\sigma(|F_o|)$. The compound forms ionic crystals which impose no crystallographic symmetry on the ions. The anion deviates somewhat from $C_{3v}$ symmetry, the $CF_3$ and $BF_3$ groups being rotated about 8° from the staggered conformation. The average C–F, B–F, and B–C bond distances are 1.343 (8) Å (corrected 1.360 Å), 1.391 (5) Å (corrected 1.409 Å), and 1.625 (6) Å (corrected 1.640 Å), respectively, the values being corrected for libration. The F–C–F angle is 104.9 (2)°. IR spectra of KBr and polyethylene pellets in the 50–2000-cm$^{-1}$ region and Raman spectra of aqueous solution, crystal powder, and single crystals were recorded on specimens with various $^{10}B$:$^{11}B$ ratios and assigned for a staggered $C_{3v}$ model. A normal-coordinate analysis yielded a general harmonic valence force field which reproduces both frequencies and observed isotope shifts and which is consistent with that of related species. The following stretching force constants were obtained: $f_{CF} = 4.85$, $f_{BF} = 4.19$, and $f_{BC} = 3.63$ mdyn/Å. Bonding in $CF_3B$ compounds is discussed on the basis of the x-ray and the spectroscopic data.

## Introduction

In preceding papers[3] we have reported the vibrational spectra of $CF_3$ derivatives of group 4–7 elements and have demonstrated the efficiency of a normal-coordinate analysis for interpretation of spectra and description of vibrational properties. The only group 3 $CF_3$ derivatives which are reported to be stable at room temperature are $CF_3BF_2$[4] and the anion $CF_3BF_3^-$.[5,6] In addition to some other physical properties, unassigned IR spectra of $CF_3BF_2$[4] and salts of the $CF_3BF_3^-$ anion[5,6] have been reported. Recently[7] $K[CF_3BF_3]$ has been thoroughly investigated by means of IR and Raman spectroscopy. We disagree with results of this investigation for three reasons. (i) The quality of the Raman spectra obtained from crystalline powder and from aqueous solutions is not acceptable; the spectra cover only the $\Delta\nu < 1300$-cm$^{-1}$ region. With one exception no depolarization ratios have been obtained. Due to the use of a wide spectral slit, some individual lines could not be resolved and no $^{10/11}B$ isotope shifts could be determined precisely. (ii) The vibration predominantly involving the $\delta_s$ $CF_3$ (umbrella) motion is always connected with an intense Ra line at 750 ± 50 cm$^{-1}$; this feature should show only a very small $^{10/11}B$ shift in $CF_3BF_3^-$. The strongest Ra line of $CF_3BF_3^-$ indeed occurs at ~730 cm$^{-1}$ and shows no shift. This line has been assigned, however, to $\nu_s$ $BF_3$ by Jackovitz et al.[7] while a band at ~970 cm$^{-1}$ with a $^{10/11}B$ shift of 22 cm$^{-1}$ has been attributed to a mode that is mainly $\nu_s$ $CF_3$ in character. Furthermore, crowding the three $a_1$ stretching vibrations in the narrow region 730–1110 cm$^{-1}$ is certainly untenable, the lowest symmetric stretch with pulsation character being expected to lie below 400 cm$^{-1}$ in $CF_3BF_3^-$ and similar systems. In addition a theoretically impossible $^{10/11}B$ shift of 50 cm$^{-1}$ has been claimed for $\nu_{as}$ $BF_3$. Why the $\nu_1$ frequency of $C_2F_6$ (this molecule is extremely useful for comparison) at 1420 cm$^{-1}$ has been disregarded, although it has never been seriously in question,[8] is not understandable.[9] (iii) Our second strongest Raman line is a sharp, polarized feature near 1350 cm$^{-1}$, which has a $^{10/11}B$ shift of 16 cm$^{-1}$ and coincides with an IR absorption. Surely this feature is an $a_1$ fundamental of $CF_3BF_3^-$. The 1100-cm$^{-1}$ region of our spectra differs considerably, being much simpler and conclusive with respect to $^{10/11}B$ shifts if the KBr pellets are prepared carefully for the IR measurements. Due to different values and assignments for several fundamentals we obtain a force field which differs from that of ref 7 but which is consistent with well-defined force fields of related species.

In addition to our vibrational spectroscopic investigation, a single-crystal x-ray study of $K[CF_3BF_3]$ is reported. The latter yielded the first structural information on group 3 $CF_3$ derivatives. Besides offering a firm structural basis for the interpretation of the vibrational spectrum, the distances and angles derived give useful clues to the bonding of $CF_3$ groups to electropositive elements.

## Experimental Section

**Preparation.** $K[CF_3BF_3]$ was prepared by the reaction of $(CH_3)_3SnCF_3$ with $BF_3$ and subsequent solvolysis with aqueous KF solution.[5] $BF_3$ was obtained by heating natural (80.4% $^{11}B$) and $^{10}B$ enriched $H_3BO_3$ (92.4% $^{10}B$; Oak Ridge National Laboratory) with an equivalent amount of $CaF_2$ and concentrated sulfuric acid in a Monel cylinder (Hoke) and was purified by a standard vacuum technique before use. Samples of $K[CF_3BF_3]$ were purified by repeated recrystallization from absolute EtOH; then larger single crystals were grown from aqueous solution.

**Infrared and Raman Spectra.** Infrared spectra of KBr (0.5–8 mg/100 mg) and polyethylene (1.5–3 mg/100 mg) pellets were recorded in the 4000–200 and 400–50-cm$^{-1}$ regions with the instruments Beckman IR 12 and Polytec FIR 30, respectively. Accuracy (not corrected for vacuum) of sharp features is ±0.5 cm$^{-1}$, resolution

**Table I.** Positional and Thermal Parameters for K[$CF_3BF_3$]

| Atom | $x$ | $y$ | $z$ | $U_{11}$[a] | $U_{22}$ | $U_{33}$ | $U_{12}$ | $U_{13}$ | $U_{23}$ |
|---|---|---|---|---|---|---|---|---|---|
| K | 0.1803 (2) | 0.1546 (1) | 0.2201 (1) | 0.0391 (6) | 0.0376 (7) | 0.0290 (6) | 0.0000 (4) | 0.0062 (4) | −0.0008 (3) |
| F(1) | 0.4957 (5) | 0.2183 (2) | −0.3896 (4) | 0.047 (1) | 0.040 (2) | 0.043 (2) | 0.012 (1) | 0.008 (1) | 0.006 (1) |
| F(2) | 0.9508 (5) | 0.1959 (2) | −0.2151 (4) | 0.043 (1) | 0.044 (2) | 0.046 (2) | −0.013 (1) | 0.000 (1) | −0.003 (1) |
| F(3) | 0.7759 (6) | 0.1365 (2) | −0.5421 (4) | 0.061 (2) | 0.048 (2) | 0.029 (1) | 0.003 (1) | 0.020 (1) | 0.001 (1) |
| F(4) | 0.5845 (7) | 0.0998 (2) | −0.0232 (4) | 0.102 (2) | 0.059 (2) | 0.034 (2) | −0.009 (2) | 0.035 (2) | 0.001 (1) |
| F(5) | 0.3683 (6) | 0.0511 (2) | −0.3230 (5) | 0.047 (2) | 0.059 (2) | 0.076 (2) | −0.023 (1) | 0.006 (1) | −0.005 (2) |
| F(6) | 0.7971 (6) | 0.0196 (2) | −0.2034 (5) | 0.066 (2) | 0.040 (2) | 0.063 (2) | 0.016 (1) | 0.017 (2) | 0.017 (1) |
| C | 0.6148 (9) | 0.0825 (3) | −0.2263 (6) | 0.040 (2) | 0.033 (2) | 0.025 (2) | 0.001 (2) | 0.006 (2) | −0.000 (2) |
| B | 0.7133 (9) | 0.1613 (3) | −0.3490 (7) | 0.035 (2) | 0.031 (3) | 0.020 (2) | 0.000 (2) | 0.006 (2) | −0.002 (2) |

[a] The form of thermal ellipsoids is $\exp[-2\pi^2(h^2a^{*2}U_{11} + k^2b^{*2}U_{22} + l^2c^{*2}U_{33} + 2hka^*b^*U_{12} + 2hla^*c^*U_{13} + 2klb^*c^*U_{23})]$.

($>650$ cm$^{-1}$) $\leq 0.6$ cm$^{-1}$, otherwise 0.6–2 cm$^{-1}$. Raman spectra of crystalline powder and solutions were obtained employing 1-mm glass capillaries, while single crystals (plates, ca. 5 × 5 × 0.5 mm) were mounted on a goniometer. A Cary 82 spectrometer was used with a $Kr^+$ laser, 647.1 nm excitation/200 mW, at the sample. Spectral slit widths were 3 cm$^{-1}$ for solutions, otherwise $\leq 2$ cm$^{-1}$; qualitative depolarization ratios are estimated.

**X-Ray Analysis. Data Collection and Reduction.** Crystals used in the x-ray investigation were cleaved from plate-like material (only the (010) face is well developed) grown from aqueous solution, examined microscopically, and attached with an epoxy resin to a glass fiber which had been mounted on a goniometer head. Crystals were examined on an automated Siemens quarter-circle diffractometer using $ZrO_2$ filtered Mo K$\alpha$ radiation and a 1° incident beam collimator. Crystal to source and crystal to detector distances were 17 and 18 cm, respectively. The pulse height analyzer was set to receive all of the Mo K$\alpha$ radiation. More than 20 specimens were found to be twinned or to give asymmetrical peak profiles. Symmetrical profiles with full widths at half-height of ~0.2° ($\omega$ scans of several strong, low-angle reflections) were given by the data crystal.

A manual search of reciprocal space ($\theta < 20°$) revealed that the crystals are monoclinic. The systematic absences $h0l$, $l = 2n + 1$, and $0k0$, $k = 2n + 1$, are unique for the space group $C_{2h}^5$-$P2_1/c$. Unit cell constants, derived by a least-squares method[12] from 35 Bragg angles ($\theta > 19°$, vertically oriented thin slit receiving collimator, $\lambda$(Mo K$\alpha_1$) 0.709 26 Å, $\lambda$(Mo K$\alpha_2$) 0.713 54 Å, $t$ 23 °C), are $a = 4.843$ (1) Å,[13] $b = 16.331$ (4) Å, $c = 6.348$ (2) Å, and $\beta = 101.89$ (3)°. The calculated density of 2.378 g cm$^{-3}$ for $Z = 4$ compares reasonably well with that observed pycnometrically in $CH_2Cl_2$, 2.5 (1) g cm$^{-3}$.

The data crystal of dimensions 0.087 × 0.551 × 0.58 mm was mounted with $c$ parallel to the $\phi$ axis. A receiving collimator having horizontal and vertical inner dimensions of 1 and 3 mm, respectively, was used. A total of 1498 reflections ($hkl$, $\bar{h}kl$, $2° \leq \theta \leq 25°$) were collected by the $\theta$–$2\theta$, five-value[14] scan technique. The Friedel equivalent of those reflections with inaccessible setting angles was measured. Symmetrical scan widths varied from 1.22 to 2.00° ($2\theta$) depending on the Bragg angle. Coincident losses were prevented and data collection time was minimized by the automatic selection of one of six Ni-foil attenuators and one of three scanning speeds, 20, 10, and 5° ($2\theta$)/min, respectively. Every 40 reflections the 0,12,0 were monitored with and without a shutter inserted in the lower half of the counter window. No intensity variation greater than $\pm 3\sigma$ was noted for this standard reflection.

Intensity data were corrected for Lorentz and polarization effects ($Lp$), monitor fluctuation, and absorption, $\mu$(Mo K$\alpha$) = 11.1 cm$^{-1}$. The transmission factor $T$ ranged from 0.506 to 0.907. The standard deviation in $|F_o|$ was estimated as $\sigma(|F_o|) = [\sigma^2(I) + (0.03I)^2]^{1/2}/(2|F_o|LpT)$, where $\sigma(I)$ is the standard deviation in the intensity $I$ as estimated by counting statistics.[14] Averaging of equivalent data yielded 864 reflections, of which 767 had $|F_o|$'s greater than $4\sigma(|F_o|)$.

**Solution and Refinement.** The structure was solved by direct methods. The sign expansion began with three origin-determining reflections and 12 symbols. This starting set was used to phase the 183 reflections with $|E| > 1.2$. The positions of the nine atoms were taken from the most probable $E$ map. The labeling of the atoms was straightforward except for the boron and carbon atoms. The naming of the latter two atoms followed from $E$-map densities [$\rho(C) > \rho(B)$] and from the average values of the shorter K–F contacts, $\langle K\text{–}F(C)\rangle > \langle K\text{–}F(B)\rangle$.

The structure was refined by least squares. The function minimized was $\sum w\Delta^2$, where $\Delta = ||F_o| - |F_c||$ and the weights $w = [\sigma^2(|F_o|) + p|F_o|^2]^{-1}$ if $|F_o| \geq 4\sigma(|F_o|)$ and $w = 0$ if $|F_o| < 4\sigma(|F_o|)$. Exponential forms of relativistic, neutral atom scattering factors were used.[15a] Real and imaginary anomalous dispersion corrections[15b] were applied for each atom. Three cycles of isotropic least-squares refinement yielded $R = \sum\Delta/\sum|F_o|$ and $R_w = [\sum w\Delta^2/\sum w|F_o|^2]^{1/2}$ of 0.123 and 0.126, respectively. Then the absorption correction was applied. Four cycles of refinement with anisotropic thermal parameters for all atoms converged with $R = 0.059$ and $R_w = 0.078$. In order to test for disorder of the C and B atoms, a double atom, constrained refinement was made. No indication of disorder was found.[16a] Examination of a function of $\langle w\Delta^2\rangle^{1/2}$ for the eight parity groups, the Miller indices, $|F_o|$, and $(\sin\theta)/\lambda$ indicated that the weights were too high for strong, low-angle reflections. A check of a $|F_o|$, $|F_c|$ list did not reveal an extinction effect. So the refinement was repeated with $p$ set to 0.0016. Then the plots of the $\langle w\Delta^2\rangle^{1/2}$ function were deemed satisfactory. The final values of $R$ and $R_w$ are 0.058 and 0.079, respectively, these summations ignoring the contribution of reflections with $|F_o| < 4\sigma(|F_o|)$. The residuals for all 864 reflections are 0.063 and 0.081, respectively. During the last cycle no parameter shifted more than 8% of its error. The largest peak, 0.71 e Å$^{-3}$, on the final difference Fourier is near the K atom. Other features ($\leq 0.46$ e Å$^{-3}$) are near K and F atoms. This residual density may be compared with the height of the B atom in this structure, 5.8 e Å$^{-3}$.[17]

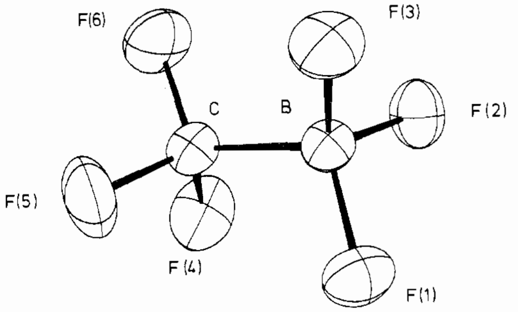

**Figure 1.** Perspective drawing of the anion of K[$CF_3BF_3$].

Positional and thermal parameters are listed in Table I, the numbering scheme being defined in Figure 1. For calculation of the errors in the anion geometry, Table II, correlation between refined parameters was taken into account. The standard deviation of interionic distances and angles, Table III, was derived from the $\sigma$'s given in Table I. Root-mean-square displacements of the atoms along their principal axes are presented in Table IV. We have attempted to fit the thermal motion of the anion atoms with a rigid body motion model.[18] The fit of 20 rigid body motion parameters to 48 temperature factors $U_{ij}$ may be judged by comparing $\{\sum[U_{ij}(\text{obsd}) - U_{ij}(\text{calcd})]^2\}^{1/2}/28 = 0.0038$ Å to $[\sum\sigma^2(U_{ij})/48]^{1/2} = 0.0015$ Å; hence while the fit seems to be fairly good, some significant nonrigid body motion may be present. The center of reaction[19] is between the C and B atoms, about 0.4 Å from the latter. The librational corrections to the C–F, B–F, and C–B bond lengths are large with respect to the errors in these values and the corrected values are also listed in Table II. No librational correction for the bond angles was felt necessary.

## Description of the Structure

**Interionic Interactions.** As expected K[$CF_3BF_3$] has been found to form an ionic solid. No crystallographic symmetry is imposed on either the anion or the cation. The crystal structure is apparently dominated by K–F interactions because the shortest interionic F–F contact—F(5)–F(6) ($x - 1, y, z$), 3.060 (4) Å —is much larger than twice the van der Waals radius of fluorine, 2.70 Å.[20] Potassium–fluorine distances less than 3.6 Å are listed in Table III. If we disregard the three longest K–F contacts, the cation is nine-coordinate. The coordination geometry may be described as a distorted square antiprism with the ninth F atom above a fourfold face. Furthermore, the formation of a short K–F contact is often accompanied by a longer, second interaction between the cation and another F atom of the same anion (Table III). If we ignore these second interactions, then the cation possesses distorted pentagonal-bipyramidal seven-coordination. The F atoms involved are indicated in Table III. The seven K–F distances range from 2.724 (3) to 2.875 (3) Å. These contacts may be compared with average K–F distances of six-coordinate and eight-coordinate potassium ions, 2.673 and 2.84 Å, respectively.[21] Interestingly, only two of these seven contacts involve F atoms of the trifluoromethyl group, and these two are the longest of the seven (Table III). The only F atom not to form a short K–F contact, F(5), also bonds to the carbon atom.

**Table II.** Bond Distances (Å) and Angles (deg) in the Anion of $K[CF_3BF_3]$

| | | | | |
|---|---|---|---|---|
| C–F(4) | 1.357 (5) | 1.374$^a$ | F(4)–C–B | 113.0 (3) |
| C–F(5) | 1.328 (5) | 1.346$^a$ | F(5)–C–B | 114.1 (3) |
| C–F(6) | 1.343 (5) | 1.359$^a$ | F(6)–C–B | 114.0 (3) |
| Av | 1.343 (8)$^b$ | 1.360 (8) | Av | 113.7 (3) |
| B–F(1) | 1.390 (5) | 1.407$^a$ | F(1)–B–F(2) | 109.8 (3) |
| B–F(2) | 1.401 (5) | 1.420$^a$ | F(1)–B–F(3) | 109.1 (3) |
| B–F(3) | 1.383 (5) | 1.400$^a$ | F(2)–B–F(3) | 110.7 (3) |
| Av | 1.391 (5) | 1.409 (6) | Av | 109.9 (5) |
| B–C | 1.625 (6) | 1.640$^a$ | F(1)–B–C | 109.5 (3) |
| ω F(3)–B–C–F(5) | −68.3$^c$ | | F(2)–B–C | 108.3 (3) |
| ω F(2)–B–C–F(6) | −68.1 | | F(3)–B–C | 109.4 (3) |
| ω F(3)–B–C–F(6) | 52.6 | | Av | 109.1 (4) |
| ω F(1)–B–C–F(4) | −68.4 | | | |
| ω F(2)–B–C–F(4) | 51.2 | | F(4)–C–F(5) | 104.9 (3) |
| ω F(1)–B–C–F(5) | 51.3 | | F(4)–C–F(6) | 104.7 (3) |
| | | | F(5)–C–F(6) | 105.2 (3) |
| | | | Av | 104.9 (2) |

[a] These distances are corrected for librational motion. [b] These are average distances. The standard deviations are calculated from the formula $[\Sigma_i(l_i - \bar{l})^2/n(n-1)]^{1/2}$. [c] These are torsional angles, a negative sign being given to those cases for which a counterclockwise rotation is required to bring the first vector into the third when viewing down the second.

**Table III.** Comparison of K–F,[a] B–F, and C–F Distances (Å) and Selected F–K–F Angles (deg)

| | | | |
|---|---|---|---|
| K–F(1)$^{\mathrm{I}\ b}$ | 2.827 (3)$^c$ | B–F(1) | 1.390 (5)$^e$ |
| K–F(1)$^{\mathrm{II}}$ | 2.750 (3)$^d$ | | |
| K–F(2)$^{\mathrm{III}}$ | 2.838 (3)$^c$ | B–F(2) | 1.401 (5) |
| K–F(2)$^{\mathrm{IV}}$ | 2.748 (3)$^d$ | | |
| K–F(3)$^{\mathrm{V}}$ | 2.724 (3)$^d$ | B–F(3) | 1.383 (5) |
| K–F(3)$^{\mathrm{I}}$ | 2.982 (3) | | |
| K–F(4) | 2.875 (3)$^d$ | C–F(4) | 1.357 (5) |
| K–F(4)$^{\mathrm{III}}$ | 3.111 (3) | | |
| K–F(5)$^{\mathrm{I}}$ | 3.319 (3) | C–F(5) | 1.328 (5) |
| K–F(6)$^{\mathrm{VI}}$ | 2.850 (3)$^d$ | C–F(6) | 1.343 (5) |

| | | | |
|---|---|---|---|
| F(1)$^{\mathrm{I}}$–K–F(1)$^{\mathrm{II}}$ | 73.5 (1) | F(2)$^{\mathrm{III}}$–K–F(2)$^{\mathrm{IV}}$ | 81.1 (1) |
| F(1)$^{\mathrm{I}}$–K–F(2)$^{\mathrm{III}}$ | 143.0 (1) | F(2)$^{\mathrm{III}}$–K–F(3)$^{\mathrm{V}}$ | 112.5 (1) |
| F(1)$^{\mathrm{I}}$–K–F(2)$^{\mathrm{IV}}$ | 82.8 (1) | F(2)$^{\mathrm{III}}$–K–F(4) | 74.0 (1) |
| F(1)$^{\mathrm{I}}$–K–F(3)$^{\mathrm{V}}$ | 82.8 (1) | F(2)$^{\mathrm{III}}$–K–F(6)$^{\mathrm{VI}}$ | 102.2 (1) |
| F(1)$^{\mathrm{I}}$–K–F(4) | 106.3 (1) | F(2)$^{\mathrm{IV}}$–K–F(3)$^{\mathrm{V}}$ | 69.8 (1) |
| F(1)$^{\mathrm{I}}$–K–F(6)$^{\mathrm{VI}}$ | 112.4 (1) | F(2)$^{\mathrm{IV}}$–K–F(4) | 134.3 (1) |
| F(1)$^{\mathrm{II}}$–K–F(2)$^{\mathrm{III}}$ | 72.6 (1) | F(2)$^{\mathrm{IV}}$–K–F(6)$^{\mathrm{VI}}$ | 155.8 (2) |
| F(1)$^{\mathrm{II}}$–K–F(2)$^{\mathrm{IV}}$ | 68.3 (1) | F(3)$^{\mathrm{V}}$–K–F(4) | 155.6 (2) |
| F(1)$^{\mathrm{II}}$–K–F(3)$^{\mathrm{V}}$ | 136.3 (1) | F(3)$^{\mathrm{V}}$–K–F(6)$^{\mathrm{VI}}$ | 87.1 (1) |
| F(1)$^{\mathrm{II}}$–K–F(4) | 67.9 (1) | F(4)–K–F(6)$^{\mathrm{VI}}$ | 68.5 (1) |
| F(1)$^{\mathrm{II}}$–K–F(6)$^{\mathrm{VI}}$ | 135.8 (1) | | |

[a] All K–F distances shorter than 3.6 Å are included. [b] Coordinates $r$ of primed atoms are related to those in the asymmetric unit as follows: $r^{\mathrm{I}} = x, y, 1 + z$; $r^{\mathrm{II}} = x, 0.5 - y, 0.5 + z$; $r^{\mathrm{III}} = x - 1, y, z$; $r^{\mathrm{IV}} = x - 1, 0.5 - y, 0.5 + z$; $r^{\mathrm{V}} = x - 1, y, 1 + z$; $r^{\mathrm{VI}} = 1 - x, -y, -z$. [c] Atom occupies an axial position of the pentagonal bipyramid of the K atom. [d] Atom occupies an equatorial position of the pentagonal bipyramid of the K atom. [e] These bond lengths are not corrected for librational shortening.

**Table IV.** Root-Mean-Square Displacements (Å) along Principal Axes in $K[CF_3BF_3]$

| Atom | Minor | Medium | Major |
|---|---|---|---|
| K | 0.17 | 0.19 | 0.20 |
| F(1) | 0.17 | 0.21 | 0.24 |
| F(2) | 0.17 | 0.22 | 0.24 |
| F(3) | 0.15 | 0.22 | 0.25 |
| F(4) | 0.15 | 0.24 | 0.32 |
| F(5) | 0.17 | 0.27 | 0.29 |
| F(6) | 0.17 | 0.24 | 0.28 |
| C | 0.16 | 0.18 | 0.20 |
| B | 0.14 | 0.18 | 0.19 |

**Anion Geometry.** While the geometry of free $CF_3BF_3^-$ is expected to possess rigorous $C_{3v}$ symmetry, the symmetry of the anion deviates clearly from $C_{3v}$ and slightly but significantly from $C_3$ in the solid state. The lowering of the symmetry from $C_{3v}$ to $C_3$ is seen in the ω (F–C–B–F) torsion angles (Table II), the $CF_3$ and $BF_3$ groups being rotated about 8° from the staggered conformation. The lowering of anion symmetry from $C_3$ to $C_1$ is revealed by $\chi^2$ tests; i.e., we can reject the hypotheses that all of the C–F bond distances and all of the F–B–F valence angles are equal at the 99% confidence level. From the list of K–F, C–F, and B–F distances in Table III, one might propose that shorter K–F distances lead to longer C–F and B–F bond lengths. However, we prefer to be cautious because $C_3$ anion symmetry would no longer be seriously questioned even in the solid state if our standard deviations were underestimated by a factor of 1.4.

The C–F bond lengths average 1.343 (8) Å (corrected 1.360 Å), and the F–C–F valence angles average 104.9 (2)°. The F–C–F angles are the smallest known to date for a trifluoromethyl group bonded to a main group element.[22] The geometry of the $CF_3$ group observed in this investigation is similar to those reported for $CF_3$ compounds of the transition elements; i.e., in $\{\eta^4\text{-}(CH_3C)_4(CF_3)Pt[P(C_6H_5)(CH_3)_2]_2\}PF_6$, ⟨C–F⟩ is 1.36 Å and ⟨F–C–F⟩ is 104°;[23] in $\eta^5\text{-}C_5H_5(CF_3)\text{-}Ni[P(C_6H_5)_3]_2$, ⟨C–F⟩ is 1.35 Å and ⟨F–C–F⟩ is 105°.[24] Using the plot of the F–C–F valence angle vs. the C–F bond length that was published by Yokozeki and Bauer[22] for 36 trifluoromethyl compounds, we calculate a C–F bond length of 1.36 Å for a F–C–F valence angle of 104.9°. The calculated length agrees particularly well with our corrected C–F bond length. The B–F bond distances and F–B–F bond angles average 1.391 (5) Å (corrected 1.409 Å) and 109.9 (5)°, respectively. Selected structural parameters for three- and four-coordinate boron compounds, containing B–F bonds, are given in Table V. Note the similarity of B–F distances in $KBF_4$,[25] $NH_4BF_4$,[26] and $K[BF_3CF_3]$. The B–C distance in $K[CF_3BF_3]$ is 1.625 (6) Å (corrected 1.640 Å). The B–C bond lengths in a number of three- and four-coordinate boron compounds are listed in Table V. Of the four-coordinate boron compounds only the B–C bond in $BH_3{\cdot}CO$, 1.54 Å,[27] deviates markedly from the value 1.64 Å. The shortness of this bond may be due in part to the sp hybridization of the carbon atom.[28] The correspondence of the B–C distances in $K[CF_3BF_3]$ and $Li[B(CH_3)_4]$ may be due to chance. The B–C bonds in the latter compound vary from 1.51 to 1.74 Å due to different types of $B\text{–}CH_3\text{–}Li$ bridging geometries.[29]

**Vibrational Spectra and Assignment.** Assuming $C_{3v}$ symmetry the isolated $CF_3BF_3^-$ anion exhibits the normal vibrations listed in Table VI. Of these the torsion $\nu_{12}$ is inactive

**Table V.** Geometry of Selected Boron Compounds

Three-Coordinate Compounds

| Compd | B–C,[a] Å | B–F, Å | ∠$C_\beta$–$C_\alpha$–$C_\beta$, deg | Ref |
|---|---|---|---|---|
| $(C_2H_3)_3B$ | $r_a$ 1.558 (3)[b] | | | 48 |
| $[C_6H_2(CH_3)_3]_3B$ | 1.575 (4) | | 117.3 (2) | 44 |
| $(C_6H_5)_3B$ | 1.577 (6) | | 116.8 (3) | 43 |
| $(CH_3)_3B$ | $r_g$ 1.578 (1)[b] | | | 45 |
| $(CH_3)_2BF$ | $r_a$ 1.55 (2)[b] | $r_a$ 1.29 (2)[b] | | 49 |
| $(C_2H)BF_2$ | $r_s$ 1.513 (5)[b] | $r_s$ 1.323 (5)[b] | | 28 |
| $(C_2H_3)BF_2$ | $r_o$ 1.532 (3) | $r_o$ 1.331 (2) | | 47 |
| $CH_3BF_2$ | $r_a$ 1.60 (3)[b] | $r_a$ 1.30 (2)[b] | | 49 |
| $BF_3$ | | 1.311 (1)[b] | | *c* |

Four-Coordinate Compounds

| Compd | B–C, Å | B–F, Å | B–D,[d] Å | ∠F–B–F, deg | Ref |
|---|---|---|---|---|---|
| $BH_3\cdot CO$ | $r_o$ 1.54 (1)[b] | | $r_o$ 1.54 (1)[b] | | 27 |
| $BF_3\cdot NC_2H_3$ | | 1.347 (6)<br>1.380 (4)[f] | 1.630 (4) | 113.0 (5) | *e* |
| $BF_3\cdot PH_3$ | | $r_s$ 1.372 (2) | $r_s$ 1.921 (7) | 112.1 (4) | *g* |
| $K[CF_3BF_3]$ | 1.625 (6)<br>1.640[h] | 1.391 (5)<br>1.409 (6)[h] | | 109.9 (5) | *i* |
| $KBF_4$ | | 1.386 (4) | | 109.4 (4) | |
| $NH_4BF_4$ | | 1.382 (6)<br>1.406 (4)[h] | | 109.4 (5) | |
| $Et_2Bpz_2^-$ | 1.620 (5)[j] | | | | |
| $Li[(CH_3)_4B]$ | 1.645 | | | | |
| $(C_6H_5)_4B^-$ | 1.642 (2)[k] | | | 114.3 (4)[k] | |

[a] The designators $r_a$, $r_g$, $r_o$, and $r_s$ define different measures of bond lengths.[22] [b] These uncertainties are error limits. [c] K. Kuchitsu and S. Konaka, *J. Chem. Phys.*, 45, 4342 (1966). [d] Donor atom of the Lewis base. [e] B. Swanson, D. F. Shriver, and J. A. Ibers, *Inorg. Chem.*, 8, 2182 (1969). [f] Bond length corrected for riding motion. [g] J. D. Odom, V. F. Kalasinsky, and J. R. Durig, *Inorg. Chem.*, 14, 2837 (1975). [h] Bond length corrected for librational motion. [i] This work. [j] The average value of the B–C bond length in the diethylbis(1-pyrazolyl)borato ($Et_2Bpz_2^-$) ligand was obtained from the following publications: B. W. Davis and N. C. Payne, *J. Organomet. Chem.*, **102**, 245 (1975); F. A. Cotton, T. La Cour, and A. G. Stanislowski, *J. Am. Chem. Soc.*, 96, 754 (1974); F. A. Cotton, B. A. Frenz, and A. G. Stanislowski, *Inorg. Chim. Acta*, 7, 503 (1973). [k] The bond length is the average of mean values found for $(C_6H_5)_4B^-$ by R. J. Sime, R. P. Dodge, A. Balkin, and D. H. Templeton, *Inorg. Chem.*, 10, 537 (1971); K. Hoffmann and E. Weiss, *J. Organomet. Chem.*, 67, 221 (1974); D. M. Duggen and D. N. Hendrickson, *Inorg. Chem.*, 13, 1911 (1974); K. J. Kruger, A. L. du Preez, and R. J. Haines, *J. Chem. Soc., Dalton Trans.*, 1302 (1974); M. Di Vaira and A. B. Orlandini, *ibid.*, 1704 (1972). The bond angle is obtained similarly from the last three publications.

**Table VI.** Number, *n*, and Distribution and Notation, *k*, of Fundamentals for the Free $CF_3BF_3^-$ Ion, for the Ion in the Crystal, and for the Unit Cell

| | | | | | Unit cell, $Z = 4$, space group $C_{2h}^5$ | | | |
|---|---|---|---|---|---|---|---|---|
| Vib mode | $a_1$ (IR, R p)[b] $n$ $(k)$[a] | $a_2$, $n$ $(k)$[a] | e(IR, R dp) $n$ $(k)$[a] | Ion in the cryst symmetry $C_1$ $n$= | $A_g$(R) $n$= | $B_g$(R) $n$= | $A_u$(IR) $n$= | $B_u$(IR) $n$= |
| $\nu$(BC) | 1 (1) | | | 1 | 1 | 1 | 1 | 1 |
| $\nu$(CF) | 1 (2) | | 1 (6) | 3 | 3 | 3 | 3 | 3 |
| $\nu$(BF) | 1 (3) | | 1 (7) | 3 | 3 | 3 | 3 | 3 |
| $\delta(CF_3)$ | 1 (4) | | 1 (8) | 3 | 3 | 3 | 3 | 3 |
| $\delta(BF_3)$ | 1 (5) | | 1 (9) | 3 | 3 | 3 | 3 | 3 |
| $\rho(CF_3)$ | | | 1 (10) | 2 | 2 | 2 | 2 | 2 |
| $\rho(BF_3)$ | | | 1 (11) | 2 | 2 | 2 | 2 | 2 |
| Torsion | | 1 (12) | | 1 | 1 | 1 | 1 | 1 |
| Librational modes | | | | | 3 | 3 | 3 | 3 |
| Translational modes | | | | | 6 | 6 | 5 | 4 |

[a] The notation *k* is not consistent with the order of frequencies $\nu_i$ in Tables VII and IX. [b] R = Raman.

both in the infrared and Raman spectrum. The site symmetry of the anion in the crystal is only $C_1$. According to Table VI the inner vibrations of the four anions in the unit cell of space group $C_{2h}^5$-$P2_1/c$ give rise to 32 Raman lines and 32 infrared bands. Table VII summarizes and Figures 2–4 reproduce the IR spectra of KBr disks and the Raman spectra obtained on aqueous solutions and single crystals with different orientation. In the crystal only the e modes $\nu_6$, $\nu_8$, $\nu_9$, $\nu_{10}$ and, to a lesser extent, $\nu_7$ are split, the relative Raman intensity of the components displaying marked orientation dependence. Hence spectra of samples with a natural abundance of B isotopes and with $^{10}B$ enriched were needed to determine $^{10/11}B$ shifts unequivocally. Precise $^{10/11}B$ shifts, which are listed in Table VIII, were determined on samples with various $^{10/11}B$ ratios; e.g., see Figure 5.

**Class $a_1$ Vibrations.** In the Raman spectrum three strong, sharp, and (in solution) polarized lines at ~1350, ~730, and ~310 cm$^{-1}$ predominate; these correspond clearly to the $a_{1g}$ vibrations of $C_2F_6$ (Table IX). Jackovitz et al.[7] have already pointed out that the intensities in the spectrum of $CF_3BF_3^-$ are those of a slightly perturbed $D_{3d}$ model. This implies that the two other $a_1$ vibrations should give rise to strong infrared bands rather than to strong Raman lines. This is in fact true for the IR/Raman pair at ~640 cm$^{-1}$ and the vibration at 1094/1066 cm$^{-1}$, which, though partly hidden by $\nu_6$ in the Raman spectrum, can be safely assigned to $\nu_2$ (vide infra). The $^{10/11}B$ shift of all $a_1$ vibrations can either be determined precisely or is smaller than the instrumental resolution. Thus, the observed shifts of the 731 and 312 cm$^{-1}$ features (less than 0.5 and 1 cm$^{-1}$, respectively) are in agreement with those

Table VII. Vibrational Spectra of $K[CF_3BF_3]$ ($cm^{-1}$)

| IR KBr/ polyethylene | Raman single crystal | Raman solution | Assign |
|---|---|---|---|
| 80 w | | | |
| 120 s | | | |
| 189 m | 190 vw | 185 vw | $\nu_{11}$ e |
| $\left.\begin{matrix}308\\315\end{matrix}\right\}$ w | 314 m | 312 s, p | $\nu_5$ $a_1$ |
| 331 w | $\left.\begin{matrix}331\\334\\342\end{matrix}\right\}$ m | 329 m, dp | $\nu_{10}$ e |
| $\left.\begin{matrix}465\\475\end{matrix}\right\}$ m | $\left.\begin{matrix}465\\475\end{matrix}\right\}$ vw | 466 vw | $\nu_9$ e |
| 560 vw | $\left.\begin{matrix}555\\559\end{matrix}\right\}$ s | 556 m, dp | $\nu_8$ e |
| | 625 vw | 625 vw | $2\nu_5$ $A_1$ |
| $\left.\begin{matrix}637.4\ {}^{11}B\\640.5\ {}^{10}B\end{matrix}\right\}$ s | $\left.\begin{matrix}639\ {}^{11}B\\643\ {}^{10}B\end{matrix}\right\}$ m | $\left.\begin{matrix}639\ {}^{11}B\\643\ {}^{10}B\end{matrix}\right\}$ w, p | $\nu_4$ $a_1$ |
| 732.0 w | 732 vs | 731 vs, p | $\nu_3$ $a_1$ |
| $\left.\begin{matrix}963\ {}^{11}B\\986\ {}^{10}B\end{matrix}\right\}$ vs | $\left.\begin{matrix}962\ {}^{11}B\\984\ {}^{10}B\end{matrix}\right\}$ vw | $\left.\begin{matrix}961\ {}^{11}B\\985\ {}^{10}B\end{matrix}\right\}$ vw | $\nu_7$ e |
| | $\left.\begin{matrix}\left.\begin{matrix}1054\\1080\end{matrix}\right\}{}^{11}B\\\left.\begin{matrix}1070\\1096\end{matrix}\right\}{}^{10}B\end{matrix}\right\}$ w | $\left.\begin{matrix}1063\ {}^{11}B\\1076\ {}^{10}B\end{matrix}\right\}$ w | $\nu_6$ e |
| $\left.\begin{matrix}1066\ {}^{11}B\\1094\ {}^{10}B\end{matrix}\right\}$ vs | $\left.\begin{matrix}1023\ {}^{11}B\\1054\ {}^{10}B\end{matrix}\right\}$ vw | | $\nu_2$ $a_1$ |
| $\left.\begin{matrix}1191\\1203\end{matrix}\right\}$ w | | | $\nu_3 + \nu_9$ E |
| $\left.\begin{matrix}1342\ {}^{11}B\\1358\ {}^{10}B\end{matrix}\right\}$ w | $\left.\begin{matrix}1343\ {}^{11}B\\1359\ {}^{10}B\end{matrix}\right\}$ m | $\left.\begin{matrix}1339\ {}^{11}B\\1356\ {}^{10}B\end{matrix}\right\}$ m, p | $\nu_1$ $a_1$ |
| $\left.\begin{matrix}1518\ {}^{11}B\\1541\ {}^{10}B\end{matrix}\right\}$ vw | | | $\nu_7 + \nu_8$ $A_1 + A_2 + E$ |

calculated by the normal-coordinate analysis.

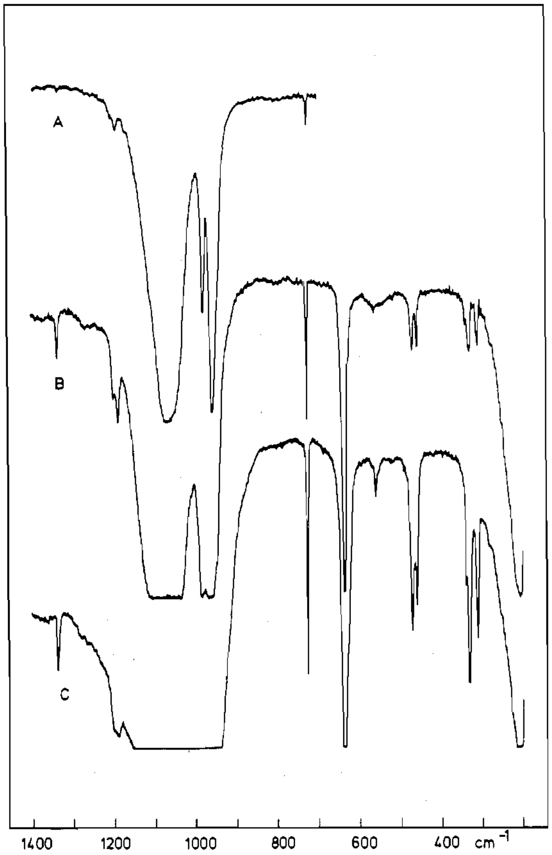

**Figure 2.** Infrared spectra of natural $K[CF_3BF_3]$: (A) KBr pellet, 0.5 mg/100 mg; (B) KBr pellet, 3 mg/100 mg; (C) KBr pellet, 8 mg/100 mg.

**Class e Vibrations.** On the basis of the similarity with the $C_2F_6$ spectrum, three e vibrations with high Raman intensity ($\nu_6$, $\nu_8$, $\nu_{10}$) and three with high IR intensity ($\nu_7$, $\nu_9$, $\nu_{11}$) are to be expected. Table IX shows that, with respect to intensity and frequency, the correspondence to the $e_g$ and $e_u$ vibrations of $C_2F_6$ is excellent. $\nu_6$, $\nu_8$, and $\nu_{10}$ fall into the regions expected for $\nu_{as}$, $\delta_{as}$, and $\rho$ $CF_3$, while $\nu_7$, $\nu_9$ and $\nu_{11}$, in accordance with

Table VIII. Observed and Calculated Frequencies, Experimental and Calculated $^{10}B/^{11}B$ Shifts (all in $cm^{-1}$), and Potential Energy Distribution $V(k)$[a]

| $\nu_{obsd}(^{11}B)$[b] | $\nu_{calcd}(^{11}B)$ | $(\Delta\nu^{10/11}B)_{exptl}$ | $(\Delta\nu^{10/11}B)_{calcd}$ | $V(k)$ ($^{11}B$) |
|---|---|---|---|---|
| $a_1$ 1339 | 1338.4 | 16 | 16.3 | 50(1), 39(2), 31(4) |
| 731 | 730.6 | <0.5 | 0.0 | 50(2), 24(4) |
| 1066 | 1063.1 | 28 | 28.7 | 43(3), 30(5), 20(2), 15(4) |
| 639 | 639.8 | 3.1 | 3.1 | 44(3), 27(5), 12(4) |
| 312 | 310.8 | <1 | 0.1 | 38(5), 34(1), 15(4) |
| e 1065 | 1066.9 | 15-16 | 15.9 | 63(6), 21(7), 21(10), 20(8), 10(11) |
| 556 | 556.6 | <1 | 0.0 | 49(8), 18(6) |
| 329 | 328.8 | <1 | 0.0 | 46(10), 39(9), 14(8), 11(11) |
| 961 | 965.0 | 23 | 22.9 | 77(7), 30(6), 16(9) |
| 466 | 467.2 | <2 | 1.4 | 47(9), 18(8), 10(7) |
| 185 | 189.4 | <1 | 0.3 | 83(11), 33(10) |

[a] $V(k) = F_{dia}L_{ik}^2 \cdot 100\Sigma_{ij}F_{ij}L_{ik}L_{jk}$ for $V(k) > 10$. [b] Solution data whenever available.

Table IX. Comparison of Selection Rules and Vibrational Intensities for $C_2F_6$ ($D_{3d}$) and $CF_3BF_3^-$ ($C_{3v}$)

| | | $C_2F_6$[8,30,a] | | | | $CF_3{}^{10}BF_3^-$ | |
|---|---|---|---|---|---|---|---|
| | | Raman | IR | | | Raman | IR |
| $a_{1g}$(R p)[c] | $\nu_1$ | 1420 m, p | | $a_1$(R p, IR) | $\nu_1$ | 1356 m, p | 1358 w |
| | $\nu_2$ | 809 vs, p | | | $\nu_3$ | 731 vs, p | 732 w |
| | $\nu_3$ | 349 s, p | | | $\nu_5$ | 312 s, p | 315 w |
| $a_{2u}$(IR) | $\nu_4$ | | 1116.9 vs | | $\nu_2$ | *d* | 1094 vs |
| | $\nu_5$ | | 714.0 vs | | $\nu_4$ | 643 w, p | 640.5 s |
| $e_g$(Rdp) | $\nu_6$ | 1237 mb | | e(R dp, IR) | $\nu_6$ | 1075 w | *d* |
| | $\nu_7$ | 620 mb | | | $\nu_8$ | 556 m | 560 vw |
| | $\nu_8$ | 380 mb | | | $\nu_{10}$ | 329 m | 331 w |
| $e_u$(IR) | $\nu_9$ | | 1250.5 vs | | $\nu_7$ | 985 vw | 986 vs |
| | $\nu_{10}$ | | 522.5 s | | $\nu_9$ | 466 vw | 465/475 m |
| | $\nu_{11}$ | | 219 s | | $\nu_{11}$ | 185 vw | 189 m |
| $a_{1u}$(inactive) | $\nu_{12}$ | | 67.5 ? | $a_2$(inactive) | $\nu_{12}$ | | *b* |

[a] J. R. Nielsen and C. M. Richards, *J. Chem. Phys.*, **16**, 67 (1948). [b] Not observed. [c] R = Raman. [d] See text.

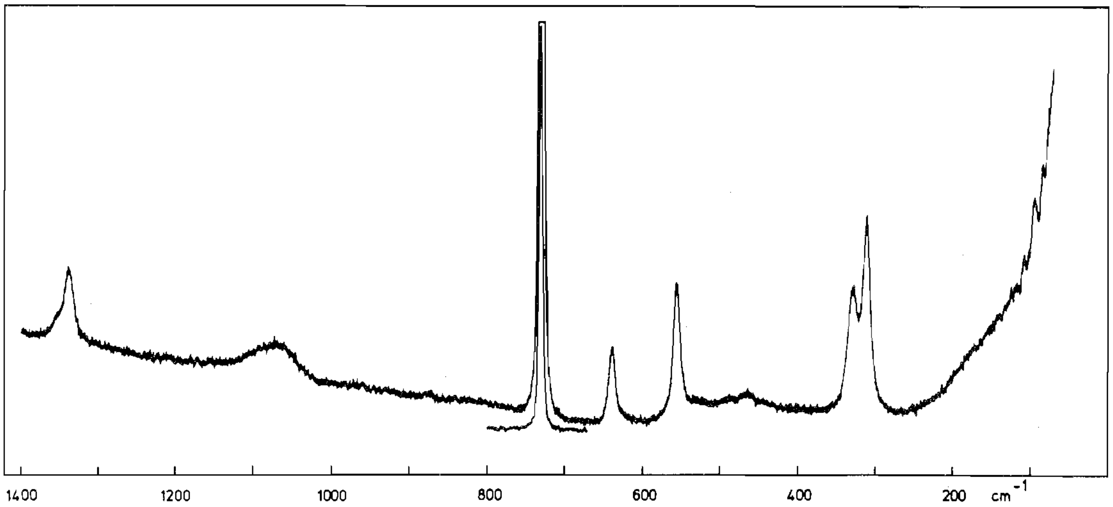

**Figure 3.** Raman spectrum of natural $K[CF_3BF_3]$, saturated aqueous solution.

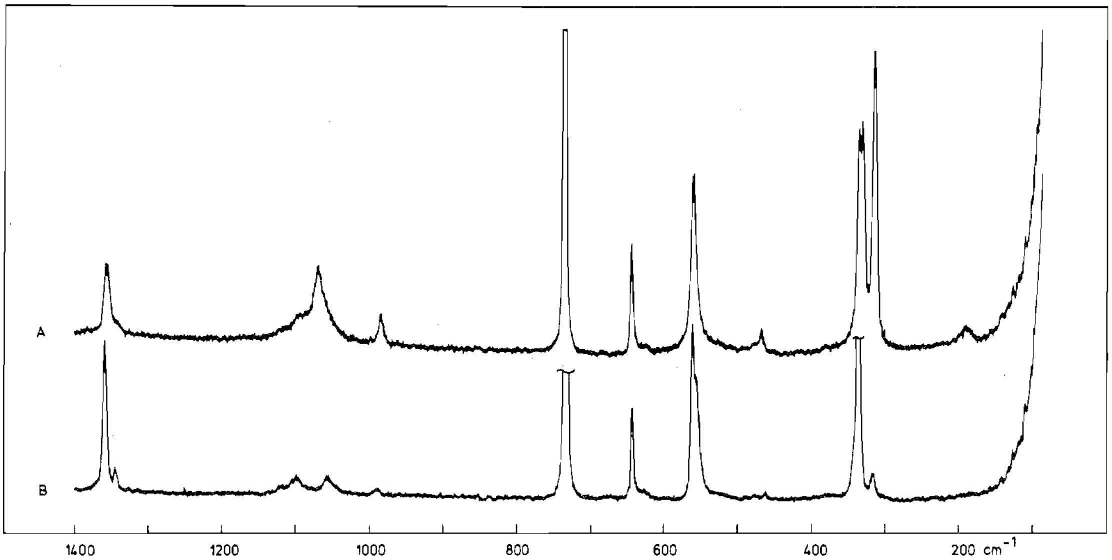

**Figure 4.** Single-crystal Raman spectra A and B of $K[CF_3BF_3]$, 92.4% $^{10}B$, recorded at different orientations of the crystal.

the normal-coordinate analysis and their $^{10/11}B$ shifts, are mainly associated with $\nu_{as}$, $\delta_{as}$, and $\rho$ $BF_3$.

Assignment of the e vibrations $\nu_7$ to $\nu_{11}$ is straightforward. Contrary to a previous observation[7] $\nu_7$ is sharp and exhibits no structure except for the isotopic splitting in the IR spectrum (Figure 5). However, the quality of the IR spectra strongly depends on the conditions under which the pellets were prepared. We admit that the conditions under which optimal disks were obtained could not always be reproduced. This concerns in particular the $\nu_2$ and $\nu_6$ region close to 1100 cm$^{-1}$ (vide infra). The assignment of $\nu_{11}$ is supported by (i) the analogy with $C_2F_6$, (ii) the fact that no Raman line in observed below 190 cm$^{-1}$, and (iii) the reasonable value of 0.69 mdyn/Å for the CBF bending force constant resulting from the normal-coordinate analysis.

The IR bands at 80 and 120 cm$^{-1}$ are presumed to be lattice modes. No evidence could be obtained for the frequency of the torsion $\nu_{12}$; this is estimated to be ≤60 cm$^{-1}$ in analogy to $C_2F_6$.[30]

**Vibrations in the 1100-cm$^{-1}$ Region.** This region is expected to contain $\nu_2$ and $\nu_6$, the vibrational character of which is related respectively to $a_{2u}$ and $e_g$ vibrations of $C_2F_6$. Hence $\nu_2$ and $\nu_6$ should be mainly IR and Raman active, respectively. Figure 5 shows the 900–1200-cm$^{-1}$ region with $\nu_2$, $\nu_6$, and $\nu_7$. The IR spectra demonstrate the change due to increasing $^{10}B$:$^{11}B$ ratio, the Raman part reproducing the tracings obtained from powder and variously oriented single-crystal specimens with the highest and lowest $^{10}B$:$^{11}B$ ratios only. The observed frequencies are listed in Table X. Presuming that the different components of the same vibration exhibit equal $^{10/11}B$ shifts, we interpret the spectra as follows. The IR spectra show two absorptions between 900 and 1200 cm$^{-1}$, only isotopic splitting being noted for samples containing boron isotopes in natural abundance. The experimental shifts for the components $y_1$ and $z_1$ are 28 and 23 cm$^{-1}$, respectively. $\nu_7$ in the powder Raman spectrum coincides with the IR frequency. Raman spectra obtained on solutions prove that the scattering near 1050 cm$^{-1}$ is depolarized. So the main components contributing to the powder and single-crystal

**Table X.** Vibrations in the $\nu_2/\nu_6/\nu_7$ Region (cm$^{-1}$)

| | $^{10}B$ | | $^{11}B$ | |
|---|---|---|---|---|
| | Raman (crystal) | IR (KBr pellet) | Raman (crystal) | IR (KBr pellet) |
| $\nu_6$ | 1096 m $^{10}x_1$ | | 1080 m $^{11}x_1$ | |
| | 1070 m $^{10}x_2$ | | 1054 m $^{11}x_2$ | |
| $\nu_2$ | | 1094 vvs $^{10}y_1$ | | 1066 vvs $^{11}y_1$ |
| | 1054 vw $^{10}y_2$ | | 1025 vw $^{11}y_2$ | |
| $\nu_7$ | 990 vw $^{10}z_1$ | | 968 vw $^{11}z_1$ | |
| | 984 vw $^{10}z_2$ | 986 vs $^{10}z_2$ | 962 vw $^{11}z_1$ | 963 vs $^{11}z_2$ |

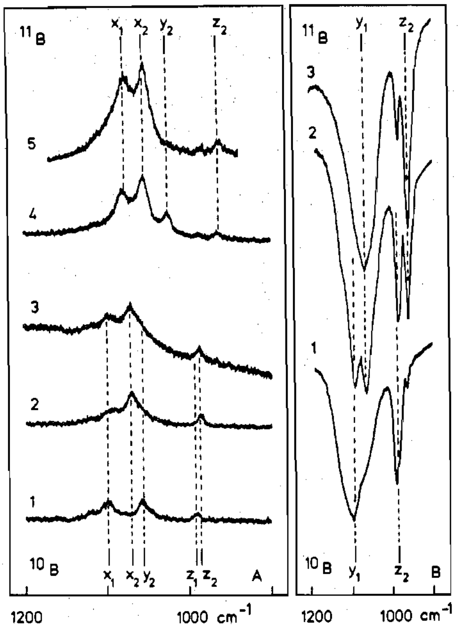

**Figure 5.** Raman and infrared spectra of K[$CF_3BF_3$] in the 900–1200-cm$^{-1}$ region: (A, Raman spectra) 1 and 2, single crystal, 92.4% $^{10}$B, different orientation; 3, crystal powder, 92.4% $^{10}$B; 4 and 5, single crystal, natural abundance, different orientation; (B, infrared spectra, KBr pellets, 0.5 mg/100 mg) 1, 92.4% $^{10}$B; 2, $^{10}$B:$^{11}$B = 1:1; 3, natural boron abundance.

spectra are likely to belong to $\nu_6$ (e) rather than to $\nu_2$ ($a_1$). This is consistent with the conclusions drawn from the analogy to $C_2F_6$.

The two bands ($^{10}x_1$, $^{10}x_2$) in the Raman powder spectrum of the $^{10}$B sample are split by 26 cm$^{-1}$; in the $^{11}$B sample $^{11}x_1$ and $^{11}x_2$ appear with the same splitting, isotopic shifts being 16 cm$^{-1}$. The latter sample, however, gives a weak, additional line $^{11}y_2$ at 1025 cm$^{-1}$. If we suppose that the component $^{11}y_2$ exhibits the same $^{10/11}$B shifts as $y_1$ does, then $^{10}y_2$ is expected to lie sufficiently close to $^{10}x_2$ to be hidden due to the low intensity of the former. The intensity ratio of the components $x_1$ and $x_2$ in the Raman spectrum depends strongly on the orientation of the crystal. At one certain orientation the $x_2$ component of a $^{10}$B sample was completely absent (Figure 5). Now $^{10}y_2$ can be clearly observed at 1054 cm$^{-1}$; the experimental shift $^{10}y_2$–$^{11}y_2$ of 29 cm$^{-1}$ is consistent with the IR shift $^{10}y_1$–$^{11}y_1$ of 28 cm$^{-1}$. Furthermore we conclude that the components $x_2$ and $y_2$ are of different symmetry. Even $z$ is likely to consist of two components, $z_1$ and $z_2$, which are, however, very close. The broadening of $^{10/11}y_1$ evident from the IR spectrum in Figure 5 is presumed to emerge from the fact that $x_1$ and $x_2$ have a significant albeit smaller intensity than $y_1$, which is situated between $x_1$ and $x_2$ for both isotopes. Similarly the sensitivity of the IR spectra in the 1100-cm$^{-1}$ region to the conditions under which the pellets are prepared may be due to such interference with components of $\nu_6$.

Solution IR spectra in $H_2O$ employing an IRTRAN 2 cell reveal an even more complex behavior. While the $^{11}$B sample exhibits one quite sharp absorption at 1082 ± 3 cm$^{-1}$, the $^{10}$B specimen shows a broad absorption at 1085 ± 5 cm$^{-1}$ as well as a shoulder of comparable intensity at 1115 ± 5 cm$^{-1}$. The $\nu_7$ absorption is sharp and located at 961 and 985 cm$^{-1}$, respectively. Obviously the ~1115-cm$^{-1}$ absorption belongs to $\nu_2$ of the $^{10}$B anion and shifts to ~1085 cm$^{-1}$ in the $^{11}$B compound. The additional feature at ~1085 cm$^{-1}$ is not sensitive to the boron mass and cannot be one of the fundamentals expected in this region. The combination bands and overtones $\nu_4 + \nu_9$ (1106/1116 cm$^{-1}$, E), $2\nu_8$ (1120 cm$^{-1}$, $A_1 + A_2 + E$), and $\nu_3 + \nu_{10}$ (1063 cm$^{-1}$, E) are close to 1085 cm$^{-1}$ and possess E components which should not interact with $\nu_2$.

**Table XI.** Nonzero Symmetry Force Constants $F_{ij}$ (mdyn/Å) of $CF_3BF_3^-$, Scaled to 1.000 Å

| $F_{ij}$, $ij$ = | | $F_{ij}$, $ij$ = | |
|---|---|---|---|
| 11 | 3.63 | 12 | 0.25 |
| 22 | 6.65 | 13 | 0.25 |
| 33 | 5.87 | 14 | −0.25 |
| 44 | 1.90 | 15 | −0.25 |
| 55 | 1.24 | 24 | 0.62 |
| 66 | 3.95 | 35 | 0.30 |
| 77 | 3.35 | 68 | −0.70 |
| 88 | 1.80 | 6,10 | 0.53 |
| 99 | 1.09 | 79 | −0.57 |
| 10,10 | 1.06 | 7,11 | 0.43 |
| 11,11 | 0.69 | 8,10 | −0.20 |
| | | 9,11 | −0.17 |
| | | 10,11 | 0.06 |

**Normal-Coordinate Analysis.** In order to gain support for the assignment, to obtain force constants for the interpretation of the bonding in the $CF_3BF_3^-$ anion, and to describe the vibrational behavior properly, a normal-coordinate analysis following the **FG** matrix method has been undertaken. A **G** matrix was calculated[31] assuming a staggered $C_{3v}$ structure with averaged bond lengths and bond angles taken from the x-ray data. A starting **F** matrix following the principle of the quadratic local symmetry force field[32] was adopted in the usual way[3] by transfer of force constants from $HCF_3$,[33] $BF_4^-$,[34] and $MeBF_2/Me_2BF$.[35] This force field reproduced both experimental frequencies and $^{10/11}$B shifts with surprising accuracy. It was refined according to the following criteria: (i) exact fit with fundamental frequencies obtained from solution spectra whenever possible, (ii) precise reproduction of experimental $^{10/11}$B shifts, (iii) reduction of the **F** matrix multiplicity according to the principle of meaningful potential energy distribution.[36]

The nonzero symmetry force constants are given by Table XI. Experimental and calculated vibrational frequencies and $^{10/11}$B shifts as well as the calculated potential energy distribution in terms of diagonal force constants are collected in Table VIII. Note that Table VIII gives the potential energy distribution in terms of diagonal force constants and not eigenvectors and, therefore, does not reflect the proper motion of the atoms. Evidently several coordinates contribute to vibrations $\nu_1$ to $\nu_{11}$. This is also implied by the pseudo-$D_{3d}$ character of the vibrational spectrum. Coupling between vibrations perpendicular to the $C_3$ axis (class e) is less pronounced than for $a_1$ vibrations. Thus it is not justified to assign the observed fundamentals to individual "CF", "BF", or "BC" vibrations.

## Discussion

The vibrational spectroscopic investigations prove a nearly ideal behavior for the $CF_3BF_3^-$ anion, namely (i) all fundamentals can be observed either in the IR and/or Raman effect, (ii) except for $2\nu_5$, $\nu_3 + \nu_9$, and $\nu_7 + \nu_9$ no overtones and combination frequencies below 2000 cm$^{-1}$ could be detected, and (iii) no evidence for anharmonic resonance was obtained. A significant result of this investigation is the unequivocal identification of $\nu_1$ and, as a consequence, that of $\nu_2$, $\nu_6$, and $\nu_7$. It does not appear possible that a combination frequency or overtone could both appear at 1340/1360 cm$^{-1}$ and exhibit a $^{10/11}$B shift of 16 cm$^{-1}$. Further disagreement with ref 7 concerns the quality of the spectra, the assignment and, consequently, the normal-coordinate analysis. We emphasize that in all cases of disagreement the results quoted in the tables are suggested by new experimental results and supported by the comparison with $C_2F_6$ and by the consistency with the x-ray results.

**Table XII.** Comparison of Force Constants (mdyn/Å)

| Compd | $f_{CF}$ | $f_{CF/CF'}$ | $f_{BF}$ | $f_{BF/BF'}$ | $f_{BC}$ |
|---|---|---|---|---|---|
| $CF_3BF_3^-$ [a] | 4.85 | 0.90 | 4.19 | 0.84 | 3.63 |
| $CF_4$ [b] | 7.32 | 0.64 | | | |
| $HCF_3$ [c] | 6.45 | 0.94 | | | |
| $HCF_3$ [d] | 6.48 | 0.82 | | | |
| $CF_3\cdot$ [e] | 6.35 | 0.84 | | | |
| $CF_3GeF_3$ [f] | 5.98 | 0.96 | | | |
| $(CH_3)_3B$ [g] | | | | | 3.64 |
| $BF_4^-$ [h] | | | 5.06 | 0.56 | |
| $BF_3$ [i] | | | 7.28 | 0.77 | |

[a] This work. [b] Reference 53. [c] Reference 33a. [d] Reference 33b. [e] Unpublished results, using $^{12}C$ and $^{13}C$ matrix frequencies from D. E. Milligan and M. E. Jacox, *J. Chem. Phys.*, 48, 2265 (1968). [f] H. Bürger and R. Eujen, *Spectrochim. Acta, Part A*, **31a**, 1645 (1975). [g] Reference 35. A BC/BC′ interaction force constant of 0.24 mdyn/Å is quoted. [h] Force constants obtained by ref 34c employing IR frequencies quoted in ref 34b. [i] J. L. Duncan, *J. Mol. Spectrosc.*, **22**, 247 (1967).

In Table XII the inner stretching force constants of $CF_3BF_3^-$ are reproduced and compared with those of related molecules. Unexpectedly, $f_{CF}$ and $f_{BF}$ are small, while at the same time $f_{CF/CF'}$ and $f_{BF/BF'}$ appear to be normal or even large. This suggests that the class e force constants $F_{66}$ and $F_{77}$, which mainly determine $\nu_6$ and $\nu_7$, could be too small. Since the ~970-cm$^{-1}$ vibration is undoubtedly the degenerate stretch $\nu_7$ and not a degenerate bending mode and since no e vibration is above 1100 cm$^{-1}$, adoption of higher values for $F_{66}$ and $F_{77}$ (and hence $f_{BC}$ and $f_{BF}$), which are also interrelated by the $^{10/11}B$ shift, appears impossible.

Despite the availability of $^{10/11}B$ shifts, B–C stretching force constants are difficult to derive precisely. This is in particular true for the $CF_3BF_3^-$ anion in which the central motion has $\nu$(BC) character. Table VIII shows that this motion contributes to several vibrations. Consequently $f_{BC}$ ($=F_{11}$) is strongly dependent on the off-diagonal elements $F_{1i}$ ($i$ = 2–5), which again are dependent on $F_{ii}$ ($i$ = 2–5). If reasonable upper limits for the interaction force constants $f_{CF/CF'}$ and $f_{BF/BF'}$ are obeyed, the BC stretching force constant $F_{11}$ lies in the range 3.0–3.8 mdyn/Å. This implies that $f_{BC}$ in $CF_3BF_3^-$ is equal or slightly (<15%) smaller than in other methylboron compounds.

Some interesting comparisons may be made between the structure of $CF_3BF_3^-$ and that of the isoelectronic hexafluoroethane molecule. First, the fact that the B–F distances in the anion are not significantly different from those in tetrafluoroborate salts is analogous to the similarity of the C–F bond lengths in $CF_4$, $r_a$ = 1.317 Å,[37] and in $CF_3CF_3$, $r_g$ = 1.326 Å.[38] The uncorrected and corrected C–F bond lengths in the anion, however, are 0.017 (8) and 0.034 (8) Å, respectively, longer compared to that in $CF_3CF_3$. Second, replacement of a carbon atom in $CF_3CF_3$ by the relatively electropositive $B^-$ would be expected[39,40] to lead to F–C–F valence angles in the anion which are smaller than those in $CF_3CF_3$, 109.1°.[38] On the average the F–C–F angle is indeed 4.2 (2)° smaller in $K[CF_3BF_3]$. In addition, the similarity between the average F–B–F angles of $K[CF_3BF_3]$ and of $KBF_4$,[25] 109.9 (5) and 109.4 (4)°, respectively, may indicate that the group electronegativity of $CF_3^-$ is comparable to the electronegativity of $F^-$. These observations based on bond angle arguments are supported by the consistency of the F–C–F and F–B–F bond angles with the C–F and B–F bond lengths, vide supra. Third, the corrected B–C distance in the anion is predicted quite well by the sum of (i) the C–C distance in $CF_3CF_3$, $r_g$ = 1.545 Å,[38] and (ii) the difference of 0.089 Å between the corrected B–F distance in the fluoroborate anion, 1.406 Å,[26] and the C–F distance in $CF_4$, 1.317 Å.[37] For comparison the difference between the tetrahedral covalent radii of B and C atoms is 0.11 Å.[20] Fourth, since the C–C distance in $CF_3CF_3$ is only 0.012 Å longer than that in $CH_3CH_3$, $r_g$ = 1.533 Å,[41] the B–C distances in $CH_3BH_3^-$ and in $CF_3BF_3^-$ might be expected to be nearly identical. This reasoning is consistent with the average B–C bond lengths observed in other[42] borate compounds (Table V) and with the lack of evidence for a fluorine substitution effect on the B–C bond length in $R_nBF_{3-n}$ ($n$ = 1–3) compounds.[46] Similarly, the B–C distance in $CH_3BF_3^-$ might be slightly shorter than that in $CF_3BF_3^-$ in analogy to the C–C distances in $CH_3CF_3$ and $CF_3CF_3$, $r_o$ = 1.530[51] and 1.545 Å,[38] respectively.

Linear correlation between C–H distances and C–H stretching force constants has been demonstrated convincingly.[52] However, comparison of Tables V and XII strongly suggests that for C–F, B–C, and B–F bonds such relation of distances (Å) and stretching force constants (mdyn/Å) does not hold. If for example the relation in $CH_nF_{4-n}$ compounds ($n$ = 0, $r_a$ = 1.317,[37] $f$ = 7.32;[53] $n$ = 1, $r_a$ = 1.334,[22] $f$ = 6.45;[33] $n$ = 2, $r_a$ = 1.360,[22] $f$ = 6.10;[54] $n$ = 3, $r_a$ = 1.391,[22] $f$ = 5.69[55]) would be applied to $CF_3BF_3^-$, the observed and corrected C–F distance (1.360 Å) suggests a force constant in the order of 6.3 mdyn/Å, while vice versa the calculated force constant (4.85 mdyn/Å) predicts a C–F bond length greater than 1.40 Å!

Previous investigations suggest that in $CF_3$ compounds $f_{CF}$ varies considerably although the C–F length is nearly constant. This suggestion is supported by transition metal $CF_3$ derivatives which have C–F bond lengths close to 1.35 Å[23,24] while $f_{CF}$ and $f_{CF/CF'}$ have been calculated to be 3.93 and 0.83 mdyn/Å, respectively, for $CF_3Co(CO)_4$.[56] Similarly we have found for $(CF_3)_2Hg$ a corrected C–F bond length of 1.349 Å, $f_{CF}$ = 5.15 mdyn/Å and $f_{CF/CF'}$ = 0.82 mdyn/Å.[57] With respect to C–F bond length and force constants, the $CF_3BF_3^-$ anion clearly compares better with transition metal $CF_3$ derivatives than with $CHF_3$. Similarly for four-coordinate boron compounds, B–F bonds show only small distance changes while the force constants vary widely.

Caution is appropriate when correlating B–C force constants and B–C bond lengths due to uncertainties quoted in previous investigations. If data so far available are considered, B–C distances in three-coordinate boron compounds are ≤1.60 Å, in borate derivatives 1.62–1.65 Å, while stretching force constants spread around 3.5 mdyn/Å in both cases. More and better structural data and improved force constants are required before conclusions can be drawn.

From the above considerations some conclusions may be drawn for the stability of trifluoromethyl compounds of boron if we assume force constants and bond lengths are related to bond strength. The C–F bonds in $K[CF_3BF_3]$ are weaker than those in $CF_4$ and $CF_3CF_3$ (indeed they seem to be weaker than those in a wide variety of $CF_3$ compounds of the main group elements[22]). Predictions from isovalent hybridization theory,[39] VSEPR theory[40] as well as the simple notion that C–F Coulombic attraction is reduced in an anion are all consistent with this observation. Were the relative weakness of the C–F bonds not offset by stronger B–C and B–F bonding, with respect to that in other borates, a degree of thermodynamic instability for $K[CF_3BF_3]$ would be implied. Although neither spectroscopic nor x-ray data imply relatively strong B–F bonding, the question of B–C bonding cannot be answered convincingly. Of course kinetic factors[5] are likely to be important to the apparent stability of $K[CF_3BF_3]$. The kinetic stability arises through the coordinate saturation of the B and C atoms; thus reaction probably is preceded by bond breaking, nucleophilic attack on the central atoms being hindered by the negatively charged F atoms. For $CF_3$ compounds of three-coordinate boron, the fourth site can receive a F atom from the $CF_3$ group, thus forming $BF_3$ and $CF_2$, as has been observed in $CF_3BF_2$.[4] The observation, however, that the reaction appears to have a significant activation energy (i.e., $CF_3BF_2$ is stable if "catalysts" are not present[4]) seems to violate this simple view. It has been proposed that F(p$\pi$) back-bonding might act to block the fourth coordination site in $CF_3BF_2$.[4] Another explanation might be that C–F bonding is stronger in $CF_3BF_2$ than in $CF_3BF_3^-$ for the same reason that the $C_\beta$–$C_\alpha$–$C_\beta$ angle is greater, ~117°, in triarylboron compounds than it is in $B(C_6H_5)_4^-$, ~114° (Table V). Clearly, more information on trifluoromethyl compounds of boron, in particular $CF_3BF_2$, is required before this problem can be settled.

Yokozeki and Bauer[22] have noted that for $(CF_3)_nA$ and $(CH_3)_nA$ compounds, the $C(CF_3)$–A distances are longer than the $C(CH_3)$–A bonds if the electronegativity of atom A is less than that of a carbon atom. The reverse is true if the electronegativity of A is greater than 2.5. Theoretical foundation for this trend has been given by CNDO calculations; as the electronegativity of A decreases, the ionic contribution to $C(CF_3)$–A bonding is no longer able to offset the loss in $C(CF_3)$–A covalent bonding relative to that in $(CH_3)_nA$ compounds.[58] Accordingly for $(CF_3)_4B^-$ and $(CH_3)_4B^-$, the $C(CF_3)$–B distance is predicted to be ~1.72 Å; i.e., 0.07–0.09 Å longer than the corresponding $C(CH_3)$–B bond. Such a prediction is inconsistent with the structure of $K[CF_3BF_3]$. Clearly there is a need to examine more $CF_3$ compounds of the more electropositive elements in order to clarify this problem.

**Acknowledgment.** Support by the Deutsche Forschungsgemeinschaft and the Ministerium für Wissenschaft und Forschung Nordrhein-Westfalen is gratefully acknowledged. We wish to thank Dr. C. Krüger, Mülheim/Ruhr, for several computer programs as well as the computer drawing.

**Registry No.** $K[CF_3BF_3]$, 42298-15-7.

**Supplementary Material Available:** A listing of structure factor amplitudes for $K[CF_3BF_3]$ (5 pages). Ordering information is given on any current masthead page.

## References and Notes

(1) Vibrational Spectra and Normal-Coordinate Analysis of $CF_3$ Compounds, 17; for part 16 see ref 2.

(2) R. Demuth, H. Bürger, G. Pawelke, and H. Willner, *Spectrochim. Acta*, in press.

(3) Leading references: (a) group 4, H. Bürger, R. Eujen, and R. J. Lagow, *Spectrochim. Acta, Part A*, **31a**, 777 (1975); H. Bürger and R. Eujen, *ibid.*, **31a**, 1655 (1975); (b) group 5, H. Bürger, R. Eujen, and R. Demuth, *ibid.*, **31a**, 1955 (1975); (c) group 6, H. Bürger and G. Pawelke, *ibid.*, **31a**, 1965 (1975); (d) group 7, A. Ruoff and H. Bürger, *Spectrochim. Acta*, in press.

(4) T. D. Parsons, J. M. Self, and L. H. Schaad, *J. Am. Chem. Soc.*, **89**, 3446 (1967).

(5) R. D. Chambers, H. C. Clark, and C. J. Willis, *Proc. Chem. Soc., London*, 114 (1960); *J. Am. Chem. Soc.*, **82**, 5298 (1960).

(6) J. Jander and H. Nagel, *Justus Liebigs Ann. Chem.*, **669**, 1 (1963).

(7) J. F. Jackovitz, C. E. Falletta, and J. C. Carter, *Appl. Spectrosc.*, **27**, 209 (1973).

(8) D. H. Rank and E. L. Pace, *J. Chem. Phys.*, **15**, 39 (1947); E. L. Pace, *J. Chem. Phys.*, **16**, 74 (1948); A. Lewis and E. L. Pace, *J. Chem. Phys.*, **58**, 3661 (1973).

(9) The gas-phase Raman spectrum of $C_2F_6$ exhibits three sharp, intense, and strongly polarized lines near 1420, 810, and 350 $cm^{-1}$ (unpublished results). The 1228-$cm^{-1}$ frequency for $\nu_1$ ($a_{1g}$) adopted by one group[10] and recommended by another[11] has never been observed and is only a guess which fits combination bands if anharmonicity is neglected.

(10) R. A. Carney, E. A. Piotrowski, A. G. Meister, J. H. Braun, and F. F. Cleveland, *J. Mol. Spectrosc.*, **7**, 209 (1961).

(11) T. Shimanouchi, *Natl. Stand. Ref. Data Ser., Natl. Bur. Stand.*, **6**, 29 (1967).

(12) In addition to local programs for the CDC 7600/7200, the programs were modified versions of Davis's LSCELD for unit cell constants; of Sheldrick's SHEL-X package for absorption correction, direct methods, least-squares, Fourier, and molecular dimensions; of Roberts and Sheldrick's XANADU for geometrical and thermal motion calculation; of Johnson's ORTEP for the drawing of the anion as well as programs written by D. J. B. for data reduction, REDUCE, and intermolecular distances and angles, ABWINK.

(13) Unless another meaning is clearly specified, a number in parentheses following a numerical value here and throughout the paper is the estimated standard deviation in the last digit.

(14) D. J. Brauer and C. Krüger, *Acta Crystallogr., Sect. B*, **29**, 1684 (1973).

(15) (a) J. A. Ibers and W. C. Hamilton, Ed., "International Tables for X-Ray Crystallography", Vol. IV, The Kynoch Press, Birmingham, 1974, Table 2.2B; (b) *ibid.*, Table 2.3.1.

(16) (a) To test for boron, carbon disorder, fractional C and B atoms were used with occupancies $\alpha$ and $1-\alpha$, respectively, at the original C atom position and $1-\alpha$ and $\alpha$, respectively, at the B atom position. Coincident atoms were constrained to have equal positional and thermal parameters. Five cycles of refinement on all parameters, starting with $\alpha = 0.5$, converged with $R = 0.058$ and $R_w = 0.0783$. No geometrical or thermal parameter shifted more than $2\sigma$. The disorder model might be accepted with a high degree of confidence since the $R$ factor ratio 0.0790/0.0783 = 1.009 is slightly larger than $R_{1,684,0.005} = 1.006$.[16b] However, the amount of disorder, $\alpha = 0.91$ (5), is not significant. The difference Fourier densities at the B atom position are −0.13 and −0.16 e $Å^{-3}$ after the ordered and disordered refinements, respectively. In both difference maps the densities at the other atom centers vary from 0.00 to 0.22 e $Å^{-3}$, background about 0.1 e $Å^{-3}$. The peak height ratio $\rho(C)/\rho(B)$ on a difference map calculated with the C and B atoms removed agrees well with the ratio observed on an electron density map calculated from the ordered model, 1.09 and 1.13, respectively. The small drop in $R_w$ during the double atom refinement, the insignificant amount of disorder indicated, and examinations of Fourier and difference Fourier maps led us to conclude that no detectable amount of disorder is present. (b) W. C. Hamilton, *Acta Crystallogr.*, **18**, 502 (1965).

(17) A listing of $|F_o|$, $F_c$ in electrons (×10) is included in supplementary material.

(18) V. Schomaker and K. N. Trueblood, *Acta Crystallogr., Sect. B*, **24**, 63 (1968).

(19) C. K. Johnson and H. A. Levy, "Thermal-Motion Analysis Using Bragg Diffraction Data", in ref 15a.

(20) L. Pauling, "The Chemical Bond", Cornell University Press, Ithaca, N.Y., 1967, p 152.

(21) K. Lonsdale, Ed., "International Tables for X-Ray Crystallography", Vol. II, The Kynoch Press, Birmingham, 1968, Table 4.1.1.

(22) A. Yokozeki and S. H. Bauer, *Top. Curr. Chem.*, **53**, 71 (1975).

(23) D. B. Crump and N. C. Payne, *Inorg. Chem.*, **12**, 1663 (1973).

(24) M. R. Churchill and T. A. O'Brien, *J. Chem. Soc. A*, 161 (1970).

(25) G. Burton, *Acta Crystallogr., Sect. B*, **25**, 2161 (1969).

(26) A. P. Caron and J. L. Ragle, *Acta Crystallogr., Sect. B*, **27**, 1102 (1971).

(27) W. Gordy, H. Ring, and A. B. Burg, *Phys. Rev.*, **78**, 512 (1950).

(28) W. J. Lafferty and J. J. Ritter, *J. Mol. Spectrosc.*, **38**, 181 (1971).

(29) D. Groves, W. Rhine, and G. D. Stucky, *J. Am. Chem. Soc.*, **93**, 1553 (1971).

(30) D. F. Eggers, R. C. Lord, and C. W. Wickstrom, *J. Mol. Spectrosc.*, **59**, 63 (1976).

(31) P. Pulay, Gy. Borossay, and F. Török, *J. Mol. Struct.*, **2**, 336 (1968); P. Pulay and W. Sawodny, *J. Mol. Spectrosc.*, **26**, 150 (1968).

(32) T. Shimanouchi in "Physical Chemistry, An Advanced Treatise", H. Eyring, D. Henderson, and W. Jost, Ed., New York, N.Y., 1970, p 233.

(33) (a) A. Ruoff, H. Bürger, and S. Biedermann, *Spectrochim. Acta, Part A*, **27a**, 1377 (1971); (b) R. W. Kirk and P. M. Wilt, *J. Mol. Spectrosc.*, **58**, 102 (1975).

(34) (a) J. Goubeau and W. Bues, *Z. Anorg. Allg. Chem.*, **268**, 221 (1952); (b) H. Bonadeo and E. Silberman, *J. Mol. Spectrosc.*, **32**, 214 (1969); (c) M. Fouassier and M. T. Forel, *ibid.*, **39**, 525 (1971).

(35) H. Siebert, *Z. Anorg. Allg. Chem.*, **268**, 13 (1952).

(36) H. J. Becher, *Fortschr. Chem. Forsch.*, **10**, 156 (1968).

(37) C. W. W. Hoffman and R. L. Livingston, *J. Chem. Phys.*, **21**, 565 (1953).

(38) K. L. Gallaher, A. Yokozeki, and S. H. Bauer, *J. Phys. Chem.*, **78**, 2389 (1974).

(39) H. A. Bent, *Chem. Rev.*, **61**, 275 (1961); A. D. Walsh, *Trans. Faraday Soc.*, **43**, 60 (1947).

(40) R. J. Gillespie, *Angew. Chem.*, **79**, 885 (1967); *Angew. Chem., Int. Ed. Engl.*, **6**, 819 (1967).

(41) K. Kuchitsu, *J. Chem. Phys.*, **49**, 4456 (1968).

(42) The B–C bond lengths in triarylboron compounds $(C_6H_5)_3B$[43] and $[C_6H_2(CH_3)_3]_3B$[44] are indistinguishable from those in $(CH_3)_3B$;[45] hence $C(sp^2)$–B and $C(sp^3)$–B distances, in $(C_6H_5)_4B^-$ and $(CH_3)_4B^-$, respectively, might also be comparable.

(43) F. Zettler, H. D. Hausen, and H. Hess, *J. Organomet. Chem.*, **72**, 157 (1974).

(44) J. F. Blount, P. Finocchiaro, D. Gust, and K. Mislow, *J. Am. Chem. Soc.*, **95**, 7019 (1973).

(45) L. S. Bartell and B. L. Carroll, *J. Chem. Phys.*, **42**, 3076 (1965).

(46) While the B–C distance in $C_2H_3BF_2$[47] is 0.026 Å shorter than that in $(C_2H_3)_3B$[48] (Table V), inspection of $C(CH_3)$–B distances in $CH_3BF_2$,[49] $(CH_3)_2BF$,[49] and $(CH_3)_3B$[45] (Table V) does not reveal any systematic trend. Also geometry-optimized ab initio MO studies[50] on $(CH_3)_nBF_{3-n}$ ($n$ = 0–3) indicate that the $C(CH_3)$–B distance is essentially unaffected by fluorine substitution.

(47) J. R. Durig, L. W. Hall, R. O. Carter, C. J. Wurrey, V. F. Kalasinky, and J. D. Odom, *J. Phys. Chem.*, **80**, 1188 (1976).

(48) A. Foord, B. Beagley, W. Reader, and J. A. Steer, *J. Mol. Struct.*, **24**, 131 (1975).

(49) S. H. Bauer and J. M. Hastings, *J. Am. Chem. Soc.*, **64**, 2686 (1942).

(50) N. F. Fitzpatrick and N. J. Mathews, *J. Organomet. Chem.*, **94**, 1 (1975).

(51) W. F. Edgell, G. B. Miller, and J. W. Amy, *J. Am. Chem. Soc.*, **79**, 2391 (1957).

(52) D. C. McKean, J. L. Duncan, and L. Batt, *Spectrochim. Acta, Part A*, **29a**, 1037 (1973).

(53) A. Ruoff, *Spectrochim. Acta, Part A*, **23a**, 2421 (1967).

(54) I. Suzuki and T. Shimanouchi, *J. Mol. Spectrosc.*, **46**, 130 (1973). They suggest that the adopted set (II) is the most likely one.

(55) J. L. Duncan, D. C. McKean, and G. K. Speirs, *Mol. Phys.*, **24**, 553 (1972).

(56) G. C. van den Berg and A. Oskam, *J. Organomet. Chem.*, **91**, 1 (1975).

(57) D. J. Brauer, H. Bürger, and R. Eujen, unpublished results.

(58) H. Oberhammer, *J. Mol. Struct.*, **28**, 349 (1975).

---

Contribution from the Departments of Chemistry,
University of Alabama, University, Alabama 35486, and Tulane University New Orleans, Louisiana 70118

# Intramolecular Hydrogen-Bonding Implications on the Lability of the Molybdenum–Piperidine Bond. Molecular Structure of *cis*-$Mo(CO)_4[P(OCH_3)_3]NHC_5H_{10}$

J. L. ATWOOD*[1] and D. J. DARENSBOURG*[2]

*Received January 13, 1977* AIC700190

The preparation of *cis*-$Mo(CO)_4[P(OCH_3)_3]NHC_5H_{10}$ by photolysis of $Mo(CO)_5P(OCH_3)_3$ in the presence of piperidine is described. The structure of this complex has been determined by single-crystal x-ray diffraction methods. The compound crystallizes in the orthorhombic space group $P2_12_12_1$ with unit cell parameters $a = 8.162$ (4) Å, $b = 11.708$ (4) Å, $c = 18.713$ (6) Å, and $\rho_{calcd} = 1.55$ g cm$^{-3}$ for $Z = 4$. Full-matrix least-squares refinement led to a final $R$ value of 2.8% based on 1422 observed reflections. The most significant structural feature of the molecule is the existence of a weak, but chemically significant, intramolecular N–H···O hydrogen bond. This interaction has been shown to greatly affect the lability of the molybdenum–piperidine bond.

## Introduction

Mechanistic studies of substitution reactions of substituted group 6B metal carbonyl derivatives have played a particularly important role in the elucidation of the details of reactions in general involving the replacement of neutral ligands from metal centers of low oxidation states.[3-7] In addition, information obtained from reactivity investigations of these octahedral complexes has been very revealing with respect to the geometry of transition states and/or intermediates involved in these ligand displacement processes.[8,9]

We have previously noted in metal carbonyl–amine complexes and related derivatives, which contain amines with the N–H grouping, that intermolecular hydrogen bonding occurs between the bound amine and donor bases (e.g., THF or $R_3P{=}O$).[6] This weak interaction was shown to result in a dissociative activation of the amine substitution process with Lewis bases. The rate enhancement for the amine displacement in the presence of donor bases was attributed to steric repulsions in the outer-sphere hydrogen-bonded intermediate as well to an increase in the effective concentration or activity of the incoming ligand at the reaction center.[7] We have therefore undertaken an investigation where the opportunity for intramolecular hydrogen bonding exists to see if there was stabilization of the metal–amine complex through hydrogen bonding. In this communication we wish to report the molecular structure of *cis*-$Mo(CO)_4[P(OCH_3)_3]NHC_5H_{10}$ in addition to spectral and amine lability studies on this species.

## Experimental Section

**Preparation of *cis*-$Mo(CO)_4[P(OCH_3)_3]NHC_5H_{10}$.** This complex was prepared in a manner similar to that previously reported.[10] $(CH_3O)_3PMo(CO)_5$[11] was irradiated in tetrahydrofuran with excess $HNC_5H_{10}$ employing a 100-W Hanovia lamp for 2 h. The solvent was removed under vacuum leaving behind a yellow oil. Upon addition of heptane yellow crystals formed which were isolated by filtration and washed several times with heptane. The complex was purified by recrystallization from chloroform/methanol. The yellow crystalline product melted with decomposition at 103–105 °C. Anal. Calcd for $Mo(CO)_4[P(OCH_3)_3]NHC_5H_{10}$: C, 34.53; H, 4.83; N, 3.36. Found: C, 34.48; H, 4.79; N, 3.39.

**Table I.** Crystal Data

| | |
|---|---|
| Compd | $Mo(CO)_4[P(OCH_3)_3]NHC_5H_{10}$ |
| Mol wt | 418.2 |
| Linear abs coeff $\mu$, cm$^{-1}$ | 8.42 |
| Calcd density, g cm$^{-3}$ | 1.55 |
| Max crystal dimensions, mm | 0.18 × 0.38 × 0.50 |
| Space group | Orthorhombic, $P2_12_12_1$ |
| Molecules/unit cell | 4 |
| Cell constants[a] | |
| *a*, Å | 8.162 (4) |
| *b*, Å | 11.708 (4) |
| *c*, Å | 18.713 (6) |
| Cell vol, Å$^3$ | 1788.2 |

[a] Mo K$\alpha$ radiation, $\lambda$ 0.710 69 Å; ambient temperature of 23 ± 1 °C.

The infrared spectrum in the $\nu$(CO) region showed bands in hexane at 2024 ($A_1$), 1928 ($A_1$), 1906 ($B_1$), and 1877 cm$^{-1}$ ($B_2$). The $\nu$(NH) vibration was observed at 3267 cm$^{-1}$ in $C_2Cl_4$.

**X-Ray Data Collection and Structure Determination for $Mo(CO)_4[P(OCH_3)_3]NHC_5H_{10}$.** Single crystals of the compound were sealed in thin-walled glass capillaries. Final lattice parameters as determined from a least-squares refinement of the angular settings for 12 reflections ($\theta > 19°$) accurately centered on the diffractometer are given in Table I. The space group was uniquely determined to be $P2_12_12_1$ [$D_2^4$, No. 19] from the systematic absences in $h00$ for $h = 2n + 1$, $0k0$ for $k = 2n + 1$, and $00l$ for $l = 2n + 1$.

Data were taken on an Enraf-Nonius CAD-4 diffractometer with graphite crystal monochromated molybdenum radiation. The diffracted intensities were collected by the $\omega$–$2\theta$ scan technique with a takeoff angle of 3.0°. The scan rate was variable and was determined by a fast (20° min$^{-1}$) prescan. Calculated speeds based on the net intensity gathered in the prescan ranged from 7 to 0.3° min$^{-1}$. Moving-crystal, moving-counter backgrounds were collected for 25% of the total scan width at each end of the scan range. For each intensity the scan width was determined by the equation

$$\text{scan range} = A + B \tan \theta$$

where $A = 0.90°$ and $B = 0.20°$. Aperture settings were determined in a like manner with $A = 4.00$ mm and $B = 2.11$ mm. Other diffractometer parameters and the method of estimation of the standard deviations have been described previously.[12] As a check on